Heat and Mass Transfer (2021) 57:1965–1979
https://doi.org/10.1007/s00231-021-03059-0

ORIGINAL

Evaluation of material property estimating methods for n-alkanes, 1-alcohols, and methyl esters for droplet evaporation calculations

Dávid Csemány [1] · István Gujás [1] · Cheng Tung Chong [2] · Viktor Józsa [1]

Received: 15 September 2020 / Accepted: 15 March 2021 / Published online: 21 May 2021

Abstract

Modeling of heat and mass transfer in liquid fuel combustion requires several material properties in a wide temperature and pressure range. The unavailable data are commonly patched with various estimation methods. In this paper, group contribution methods (GCM) and law of corresponding states (LCS) were analyzed for estimating material properties of n-alkanes (up to $C_{10}H_{22}$ and $C_{12}H_{26}$), 1-alcohols (up to $C_{10}H_{22}O$), and methyl esters (up to $C_{19}H_{38}O_2$ and $C_{19}H_{36}O_2$). These were compared to reference data to evaluate their applicability. LCS suggested by Poling et al. provides proper estimation for the acentric factor. GCM of Joback accurately estimates normal boiling point, critical properties, and specific heat capacity of the vapor-phase, the latter was corrected for methanol, however, GCM of Constantinou is more accurate for critical pressure of methyl esters. GCM of Ruzicka is suitable for estimating liquid-phase specific heat capacity. This method was updated for methanol. GCM of Elbro gives a proper estimation for liquid-phase density, while LCS of Lucas estimates vapor-phase viscosity properly. LCS of Chung and the modified Eucken method for vapor-phase and GCM of Sastri for liquid-phase thermal conductivity are appropriate. Considering the gas-phase mutual diffusion coefficient, the method of Fuller provides the best estimation, while LCS methods of Riedel and Chen are suitable for the enthalpy of vaporization at the normal boiling point.

Keywords Material data · Evaporation · Liquid combustion · N-alkane · Alcohol · Methyl ester

NomenclatureLatin letters

ARD	Average relative deviation, %
c_p	Specific heat capacity at constant pressure, J/(kg·K)
c_v	Specific heat capacity at constant volume, J/(mol·K)
D_{12}	Gas-phase mutual diffusion coefficient, m^2/s
H	Enthalpy of vaporization, J/kg
k	Thermal conductivity, W/(m·K)
M	Molecular mass, kg/kmol
p	Pressure, bar
$\Re$	Universal gas constant (8.314 kJ/(kmol·K))
T	Temperature, K
V	Volume, cm^3/mol

There are several constants used in the equations which are noted at their first occurrence and are used only locally.

Greek symbols

μ	Dynamic viscosity, Pa·s
ρ	Density, kg/m^3
σ	Deviation
ω	Acentric factor, 1

Subscripts

bn	Boiling point at 101,325 Pa
c	Critical
est	Estimation
l	Liquid
r	Reduced value
ref	Reference
T	Temperature
v	Vapor

✉ Dávid Csemány
csemany@energia.bme.hu

István Gujás
gujasistvan@gmail.com

Cheng Tung Chong
ctchong@sjtu.edu.cn

Viktor Józsa
jozsa@energia.bme.hu

[1] Department of Energy Engineering, Faculty of Mechanical Engineering, Budapest University of Technology and Economics, Műegyetem rkp. 3., Budapest H-1111, Hungary

[2] China-UK Low Carbon College, Shanghai Jiao Tong University, Lingang, Shanghai 201306, China

1 Introduction

Biomass-to-fuel conversion methods have attracted numerous theoretical and practical research in the past few decades with special emphasis on the transportation sector [1, 2]. There are numerous ways available to produce biofuels. Short- and long-chain n-alkanes can be produced from synthesis gas by chemo- and biocatalytic processes [3, 4]. The main source of alcohols is fermentation which provides positive energy balance [5, 6]. It is known that alcohol/diesel blend utilization improves the performance and lowers the pollutant emissions of internal combustion engines [7, 8]. Methyl esters are produced from fats and vegetable oils by esterification and mainly used in biodiesel fuels as a renewable additive to diesel oil, thus information on material properties is indispensable [9, 10]. The present paper deals with the three molecular groups due to their dominance in the renewable fuel industry [11, 12].

Upon selecting the principal characteristics, nowadays, combustion chamber design for liquid fuels starts with numerical analysis, including all the major heat and mass transfer processes [13–15]. Then the results are validated by experiments [16, 17]. Nevertheless, modeling the heat and mass transfer of a real multicomponent or nanofluid [18] fuels is still challenging [19, 20] since the majority of the used material property models are not validated in a practically adequate extent.

Modeling heat and mass transfer requires the knowledge of several thermodynamic properties [21]. Some of them are constant, e.g., critical temperature, pressure, volume, and normal boiling point. Others depend on the thermodynamic conditions, they are, e.g., specific heat capacity and thermal conductivity of both the liquid and vapor phases, liquid density, vapor viscosity, gas-phase mutual diffusion coefficient of fuel vapor and the ambient gas, and enthalpy of vaporization. Therefore, they have a significant influence on model sensitivity and validation [22]. The most notable difficulty in practice is that the above-mentioned data are highly limited. Unfortunately, the limitations of these methods are seldom discussed with the engineer who runs a commercial software code that relies on these estimations.

The present study reviews the available pure component material property estimating methods required for calculating the evaporation of a droplet which are mainly discussed in ref. [23]. Su et al. [24] also provide a comprehensive review for the available estimating techniques with the originally published statistical parameters to predict their accuracy for several material properties. The motivation of the present study originates from combustion, hence, estimating methods for material properties required for heat and mass transfer calculations are emphasized. These approaches all rely on molecular theory, aiming to be as general as reasonable which does not necessarily work for all materials. More precisely, there are flaws even for a series of simple hydrocarbons. Consequently, there are a few different methods available for the calculation of a single material property. Note that other molecules, e.g., branched alkanes and cyclic compounds are also relevant in combustion technology. However, reliable reference data for them in terms of all the necessary material properties are often unavailable or limited to narrow ambient conditions. Hence, this paper evaluates solely n-alkanes, 1-alcohols, and methyl esters, focusing on parameters influencing droplet evaporation.

2 Models

The evaluated material property estimating methods are discussed next, highlighting the key equations only. Their theoretical background is available for the reader in the cited references nearby. These models can be divided into two main groups. The first one is using the law of corresponding states (LCS), and the other is relying on the group contribution method (GCM) [23]. According to LCS, the equilibrium properties, which are depending on intermolecular forces, are related to the critical properties. Therefore, pressures, volumes, and temperatures are discussed as reduced values (e.g., pressure divided by the critical pressure) and assumed as identical for all fluids, thus properties can be determined in terms of the critical parameters with general empirical models. Consequently, LCS works well mostly for simple molecules. However, improved accuracy can be reached by adding extra parameters which characterize the molecular structure, such as acentric factor for weakly polar and dipole moment for strongly polar molecules, and semi-empirical constants based on measurement data. GCM is relying on the following philosophy. Molecular structure and intermolecular bonds determine the intermolecular forces which is the governing factor of the macroscopic properties. This approach uses weighting factors for atoms, functional groups, and bond types, and their contributions are summed, then the result is empirically corrected. The contributions are determined from reference data by a suitable optimization procedure. Therefore, a comprehensive measurement database is required in terms of molecule types and chain lengths in order to provide a sufficiently accurate and general method. The investigated models were chosen because of their simplicity and general applicability, however, improved variants are available in the literature [25]. In a practical application like combustion the more general formulation due to the wide temperature and pressure range and the low computational demand are essential for solving a large set of equations at millions of nodes simultaneously [26]. The evaluated estimation methods are discussed below for the relevant material properties of liquid evaporation.

2.1 Acentric factor

The acentric factor, ω, was originally introduced by Pitzer et al. [27], using LCS. The slope of the vapor pressure curve is

related to the entropy of vaporization, hence they regarded ω as a measure of the increase in the entropy of vaporization over that of a simple fluid. For a simple fluid the reduced vapor pressure, $p_{vr} = p_v/p_c$ is almost accurately 0.1 at a reduced temperature, $T_r = T/T_c = 0.7$, where p_v, p_c, and T_c are vapor pressure, critical pressure, and critical temperature, respectively. Pitzer et al. [27] considered this point on the vapor pressure curve to determine the acentric factor because it is far enough from the critical point and above the melting point for nearly all materials. Therefore, their original definition is the following:

$$\omega = -\log_{10} p_{vr,0.7} - 1, \tag{1}$$

where $p_{vr,0.7}$ is the reduced vapor pressure at $T_r = 0.7$. Poling et al. [23] suggested the following equation for the acentric factor:

$$\omega = -\left[\ln\left(\frac{p_c}{1.01325}\right) + f^{(0)}\right]/f^{(1)}, \tag{2}$$

where both $f^{(0)}$ and $f^{(1)}$ are functions of the normal boiling temperature, T_{bn}, and critical temperature, developed by Ambrose [28]. Equation (2) results from ignoring the term ω^2 in the original Pitzer expansion and solving for ω [23]. Constantinou et al. [29] developed a GCM-based approach for calculating ω:

$$\omega = 0.4085 \cdot [\ln(1.1507 + \textstyle\sum_k N_k \cdot w_k)]^{1/0.5050}, \tag{3}$$

where N_k and w_k are the number and weighting factors of the k^{th} group, respectively.

2.2 Normal boiling point and critical properties

Joback [30, 31] reevaluated the existing GCM schemes for T_{bn}, T_c, p_c, and critical volume, V_c, and determined the following equations:

$$T_{bn} = 198 + \textstyle\sum_k N_k \cdot tbn_k, \tag{4}$$

$$T_c = T_{bn} \cdot \left[0.584 + 0.965 \cdot \{\textstyle\sum_k N_k \cdot tc_k\} - \{\textstyle\sum_k N_k \cdot tc_k\}^2\right]^{-1}, \tag{5}$$

$$p_c = [0.113 + 0.0032 \cdot N_{atom} - \textstyle\sum_k N_k \cdot pc_k]^{-2}, \tag{6}$$

$$V_c = 17.5 + \textstyle\sum_k N_k \cdot vc_k, \tag{7}$$

where tbn_k, tc_k, pc_k, and vc_k are the weighting factors for T_{bn}, T_c, p_c and V_c, respectively. N_{atom} is the number of atoms in the molecule. Constantinou et al. [29, 32] also developed a GCM-based estimation method for the critical parameters and normal boiling point, using another functions:

$$T_{bn} = 204.359 \cdot \ln\left(\textstyle\sum_k N_k \cdot \widetilde{tbn_k}\right), \tag{8}$$

$$T_c = 181.128 \cdot \ln\left(\textstyle\sum_k N_k \cdot \widetilde{tc_k}\right), \tag{9}$$

$$p_c = \left[0.10022 + \textstyle\sum_k N_k \cdot \widetilde{pc_k}\right]^{-2} + 1.3705, \tag{10}$$

$$V_c = 1000 \cdot \left(-0.00435 + \textstyle\sum_k N_k \cdot \widetilde{vc_k}\right), \tag{11}$$

where the tbn_k, tc_k, pc_k, and vc_k constants with tilde differ from the ones used in Eqs. (4)–(7). Nevertheless, they bear a similar meaning.

2.3 Specific heat capacity of the vapor

Assuming that the vapor-phase of a substance can be modeled as an ideal gas at atmospheric pressure, Joback [30, 31] and Nielsen [33] derived the following equations for the specific heat capacity of the vapor, defined by Eqs. (12) and (13):

$$c_{p,v} = \begin{pmatrix} \sum_k N_k \cdot C_pA_k - 37.93 + \left[\sum_k N_k \cdot C_pB_k + 0.21\right] \cdot T \\ + \left[\sum_k N_k \cdot C_pC_k - 3.91 \cdot 10^{-4}\right] \cdot T^2 \\ + \left[\sum_k N_k \cdot C_pD_k + 2.06 \cdot 10^{-7}\right] \cdot T^3 \end{pmatrix} \cdot 10^3/M, \tag{12}$$

$$c_{p,v} = \begin{pmatrix} \sum_k N_k \cdot \widetilde{C_pA_k} - 19.7779 \\ + \left[\sum_k N_k \cdot \widetilde{C_pB_k} + 22.5981\right] \cdot (T-298)/700 \\ + \left[\sum_k N_k \cdot \widetilde{C_pC_k} - 10.7983\right] \cdot [(T-298)/700]^2 \end{pmatrix} \cdot 10^3/M, \tag{13}$$

where C_pA_k, C_pB_k, C_pC_k, and C_pD_k are the contribution constants of the k^{th} relevant group and M is the molecular mass. The tilde differentiates the constants used by the two models. Note that Nielsen [33] used the same group contributions determined by Constantinou [29, 32].

2.4 Liquid specific heat capacity

Ruzicka and Domalski [34] proposed a GCM to calculate the specific heat capacity of liquids, $c_{p,l}$, from the melting point to the boiling point:

$$c_{p,l} = \frac{1000 \cdot \Re}{M}\left[\textstyle\sum_k N_k \cdot a_k + \frac{T}{100} \cdot \sum_k N_k \cdot b_k + \left(\frac{T}{100}\right)^2 \cdot \sum_k N_k \cdot d_k\right], \tag{14}$$

where a_k, b_k, and d_k are the contribution constants of the k^{th} relevant group, and $\Re$ is the universal gas constant. Another method was proposed by Poling et al. [23] who revised the LCS of Bondi [35] for calculating $c_{p,l}$:

$$c_{p,l} = \left\{1.586 + \frac{0.49}{1-T_r} + \omega \cdot \left[4.2775 + \frac{6.3 \cdot (1-T_r)^{1/3}}{T_r} + \frac{0.4355}{1-T_r}\right]\right\} \cdot \Re \cdot \frac{1000}{M} + c_{p,v} \tag{15}$$

2.5 Vapor dynamic viscosity

LCS of Chung et al. [36, 37] relates the Lennard-Jones potential parameters to macroscopic parameters in order to determine dynamic viscosity of the vapor, μ_v, according to Eq. (16):

$$\mu_v = 40.785 \cdot \frac{F_c \cdot (M \cdot T)^{1/2}}{V_c^{2/3} \cdot \Omega_v} \cdot 10^{-7}, \tag{16}$$

where F_c is the function of ω and dipole moment, and Ω_v is the viscosity collision integral which is the function of T_r. Another LCS from Lucas [38] has been investigated for the estimation of μ_v, defined by Eq. (17):

$$\mu_v = 5.682 \cdot 10^{-7} \cdot \left[0.807 \cdot T_r^{0.618} - 0.357 \cdot e^{-0.449 \cdot T_r} + 0.34 \cdot e^{-4.058 \cdot T_r} + 0.018\right] \cdot F_P^o \cdot \left(\frac{T_c}{M^3 \cdot p_c^4}\right)^{-1/6}, \tag{17}$$

where the value of $F_P{}^O$ is the function of the dipole moment, p_c, and T_c.

2.6 Vapor thermal conductivity

Chung et al. [36, 37] applied LCS to obtain the thermal conductivity of the vapor-phase, k_v, defined by Eq. (18):

$$k_v = \frac{3.75 \cdot \Psi \cdot \Re \cdot \mu_v}{M \cdot 10^{-3}}, \tag{18}$$

where Ψ is a function of $c_{p,v}$, ω, and T_r. Equation (19) is the popular Eucken method [23], an alternative way to estimate k_v. Equation (19) was modified by Svehla [39] as Eq. (20), and Stiel and Thodos [40] also proposed a correction, defined by Eq. (21):

$$k_v = \frac{\mu_v \cdot c_{v,v}}{M \cdot 10^{-3}} \cdot \left(1 + \frac{9/4}{c_{v,v}/\Re}\right), \tag{19}$$

$$k_v = \frac{\mu_v \cdot c_{v,v}}{M \cdot 10^{-3}} \cdot \left(1.32 + \frac{1.77}{c_{v,v}/\Re}\right), \tag{20}$$

$$k_v = \frac{\mu_v \cdot c_{v,v}}{M \cdot 10^{-3}} \cdot \left(1.15 + \frac{2.03}{c_{v,v}/\Re}\right), \tag{21}$$

where $c_{v,v}$ is the constant volume specific heat capacity of the vapor.

2.7 Liquid thermal conductivity

The estimation methods for the liquid thermal conductivity, k_l, are extensively empirical, therefore, testing and validating them is mandatory. Equation (22) was developed by Latini and Pacetti [41]:

$$k_l = \frac{A \cdot T_b^{\alpha} \cdot (1 - T_r)^{0.38}}{M^{\beta} \cdot T_c^{\gamma} \cdot T_r^{1/6}}, \tag{22}$$

where A, α, β, and γ are constants, depending on the type of the molecule. Sastri and Rao [42, 43] recommended two GCMs, defined by Eqs. (23) and (24):

$$k_l = a^{1-\left(\frac{1-T_r}{1-T_{br}}\right)^n} \cdot \sum_k N_k \cdot \Delta k_k, \tag{23}$$

$$k_l = \left(\frac{T_{bn}}{T}\right)^{1/2} \cdot \sum_k N_k \cdot \Delta k_k, \quad \text{where } T < T_{bn} \tag{24}$$

where a and n are constants, depending on the molecule type. $T_{br} = T_{bn}/T_c$ and Δk_k is the contribution constants of the k^{th} relevant group.

2.8 Liquid density

Two GCMs for estimating liquid density, ρ_l, have been investigated. Baum [44] suggested Eq. (25):

$$\rho_l = \frac{1000 \cdot M}{\sum_k n_k \cdot v_k} \cdot \left(3 - 2 \cdot \frac{T}{T_{bn}}\right)^n, \tag{25}$$

where n is a constant, depending on the molecule type, and v_k is the contribution constants of the k^{th} relevant atom in the molecule. Eq. (26) was obtained by Elbro et al. [45]:

$$\rho_l = \frac{1000 \cdot M}{\sum_k n_k \cdot \left(A_k + B_k \cdot T + C_k \cdot T^2\right)}, \tag{26}$$

where A_k, B_k, and C_k are the contribution constants of the k^{th} relevant groups.

2.9 Gas-phase mutual diffusion coefficient

The gas-phase mutual or binary diffusion coefficient, D_{12}, refers to the diffusion in a binary system consisting of constituents 1 and 2. The classical Chapman-Enskog formula [23] is defined by Eq. (27):

$$D_{12} = \frac{0.00266 \cdot T^{3/2}}{p \cdot M_{12}^{1/2} \cdot \sigma_{12}^2 \cdot \Omega_D} \cdot 10^{-4}, \tag{27}$$

where σ_{12} is the average Lennard-Jones characteristic length of the constituents, M_{12} is the average molecular mass, and Ω_D is the diffusion collision integral, which is the function of T and the average Lennard-Jones characteristic energy of the constituents. Equation (27) has been empirically modified by Wilke [46] and Fuller et al. [47, 48], leading to Eqs. (28) and (29), respectively:

$$D_{12} = \frac{\left(3.03 - \frac{0.98}{M_{12}^{1/2}}\right) \cdot 10^{-3} \cdot T^{3/2}}{p \cdot M_{12}^{1/2} \cdot \sigma_{12}^2 \cdot \Omega_D} \cdot 10^{-4}, \tag{28}$$

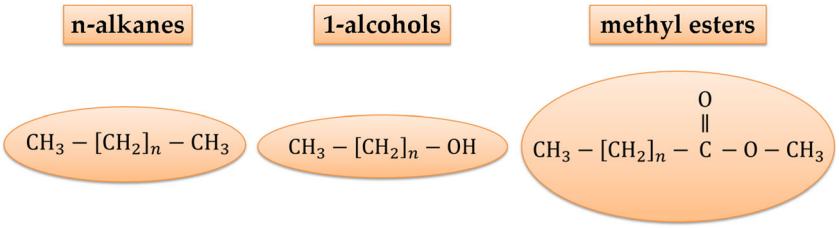

Fig. 1 The general structure of the investigated materials

$$D_{12}=\frac{0.00143\cdot T^{7/4}}{p\cdot M_{12}^{1/2}\cdot\left[(\Sigma_v)_1^{1/3}+(\Sigma_v)_2^{1/3}\right]^2}\cdot 10^{-4}, \tag{29}$$

where Σ_v is the sum of atomic and structural diffusion volume increments of the corresponding molecules.

2.10 Enthalpy of vaporization at the normal boiling point

Calculating the latent heat of vaporization is often necessary in heat and mass transfer problems. The Watson relation [23, 49] is frequently used for this purpose, where the enthalpy of vaporization is an input parameter. When atmospheric conditions are considered, enthalpy of vaporization at the normal boiling point is required. Riedel [50], Chen [51], and Vetere [52] correlated the enthalpy of vaporization with the critical parameters by LCS, leading to Eqs. (30), (31), and (32), respectively when applied to the normal boiling point:

$$H_{T_{bn}}=1093\cdot\Re\cdot T_c\cdot T_{br}\cdot\frac{\ln p_c-1.013}{(0.93-T_{br})\cdot M}, \tag{30}$$

$$H_{T_{bn}}=1000\cdot\Re\cdot T_c\cdot T_{br}\cdot\frac{3.978\cdot T_{br}-3.958+1.555\cdot\ln p_c}{(1.07-T_{br})\cdot M}, \tag{31}$$

$$H_{T_{bn}}=1000\cdot\Re\cdot T_{bn}\frac{(1-T_{br})^{0.38}\cdot\left[\ln p_c-0.513+0.5066/\left(p_c\cdot T_{br}^2\right)\right]}{\left\{1-T_{br}+F\cdot\left[1-(1-T_{br})^{0.38}\right]\cdot\ln T_{br}\right\}\cdot M}, \tag{32}$$

where $F=1$, except for alcohols with more than two carbon atoms.

3 Materials

The investigated materials are summarized next. Their evaluated material properties were gathered principally from the NIST [53] and other databases [23, 54, 55]. However, ref. [54] was only used for the normal boiling points of longer-chain methyl esters (from C_{13} to C_{19}), 10 data points for liquid-phase density of 1-alcohols (from C_2 to C_{10}), and 11 data points for liquid-phase density of methyl esters (from C_3 to $C_{19:1}$), but only at room temperature, where reference data were considered reliable. Ref. [54] refers to National Oceanic and Atmospheric Administration's Office of Response and Restoration - Cameo Chemicals Database of Hazardous Materials [56] in case of liquid density of C_6–C_7 methyl esters and to National Library of Medicine of the National Institutes of Health - Hazardous Substances Data Bank (HSDB) [57] in case of the other data points. Ref. [54] also indicates the details of the original references for all the individual data points found in HSDB and Cameo Chemicals Database. For further information, the reader is directed to ref. [54]. Material properties from the NIST [53] and refs. [23, 54] databases were used as reference values at atmospheric pressure, except for the gas-phase mutual diffusion coefficient which was obtained from ref. [55]. For the gas-phase mutual diffusion coefficient, both atmospheric and elevated pressures were investigated. D_{12} was available for

Table 1 Relevant groups of the investigated materials for each GCM. Superscripts refer to the functional groups present in 1: n-alkanes, 2: 1-alcohols, and 3: methyl esters

T_{bn}, T_c, p_c, V_c, $c_{p,v}$ - Joback [30, 31]	$CH_2^{1,2,3}$, $CH_3^{1,2,3}$, OH^2, COO^3, $CH=^3$
ω, T_{bn}, T_c, p_c, V_c, – Constantinou et al. [29, 32]	$CH_2^{1,2,3}$, $CH_3^{1,2,3}$, OH^2, CH_3COO^3, $CH=CH^3$
$c_{p,v}$ - Nielsen [33]	$CH_2^{1,2,3}$, $CH_3^{1,2,3}$, OH^2, CH_3COO^3
$c_{p,l}$ - Ruzicka [34]	C-(2H,2C) ^{1,2,3}, C-(3H,C) ^{1,2,3}, C-(2H,C,O) ^{2}, O-(H,C) ^{2}, C-(2H,C,CO) ^{3}, CO-(C,O) ^{3}, O-(C,CO) ^{3}
k_l - Sastri [43]	H^1,>C<^{1}, CH_2^1, CH_3^1
ρ_l - Baum [44]	$C^{1,2,3}$, $H^{1,2,3}$, $O^{2,3}$
ρ_l - Elbro et al. [45]	$CH_2^{1,2,3}$, $CH_3^{1,2,3}$, CH_2OH^2, CH_3COO^3, $CH=^3$
D_{12} - Fuller et al. [47, 48]	$C^{1,2,3}$, $H^{1,2,3}$, $O^{2,3}$

Table 2 The relative uncertainty of the material properties of the investigated fluids, obtained from the NIST database [53] and ref. [55]

	$\sigma T_{bn}/T_{bn}$	$\sigma T_c/T_c$	$\sigma p_c/p_c$	$\sigma V_c/V_c$	$\sigma\rho/\rho$	$\sigma c_p/c_p$	$\sigma k/k$	$\sigma\mu/\mu$	$\sigma D_{12}/D_{12}$	$\sigma H_{Tbn}/H_{Tbn}$
n-alkanes	<2%	<1%	<5%	1–7%	<2%	1–5%	2–5%	2–5%	<2%	1%
1-alcohols	<2%	<4%	1–10%	<4%	<1%	<1%	–	–	10%	1%
methyl esters	1–10%	1–6%	–	–	–	<1%	–	–	14%	1%

methanol and ethanol at high pressures, up to 100 bar, as well. Homologous series of n-alkanes from methane (CH_4) to decane ($C_{10}H_{22}$) and dodecane ($C_{12}H_{26}$) were investigated as this range is of great relevance in practical combustion chambers, as the kinetics of fuel thermal cracking to form smaller molecular fragments is fast in high-temperature environments [58, 59]. Moreover, C_5–C_{12}, C_8–C_{16}, and C_{10}–C_{22} n-alkanes are present in gasoline, kerosene, and diesel fuels, respectively [4]. However, reliable temperature-dependent reference data for the estimated material properties were only available up to $C_{12}H_{26}$. Furthermore, homologous series of primary alcohols from methanol (CH_4O) to decanol ($C_{10}H_{22}O$) and methyl esters from methyl ethanoate ($C_3H_6O_2$) to methyl stearate ($C_{19}H_{38}O_2$) and methyl oleate ($C_{19}H_{36}O_2$) were evaluated due to the scarce data for higher carbon numbers. Besides their direct utilization, they are often used in surrogate mixtures of conventional and renewable fuels. Moreover, these compounds are typically used for construction of reaction mechanisms and combustion simulations, where thermodynamic properties are often needed. Figure 1 shows the general structure of the investigated materials. Note that methyl oleate ($C_{19}H_{36}O_2$) has a CH=CH double bond, thus the structure is different from the saturated hydrocarbon chain shown in Fig. 1. However, it is the only molecule with unsaturated hydrocarbon chain discussed in the present paper. Reference data was available for the acentric factor, critical properties, T_{bn}, $c_{p,v}$, $c_{p,l}$, ρ_l, D_{12}, and H_{Tbn} for all three types of molecules. k_v, k_l, and μ_v were only available for n-alkanes. Table 1 contains the relevant groups of the investigated materials for each GCM, and Table 2 contains the corresponding uncertainties of the reference data, where it was available. Table 3 contains the availability of the reference data. This dataset is accessible in the following online repository [60].

4 Results and discussion

The comparison of the estimating methods and the reference data is analyzed in the present section. For reference, the relative deviation of ±5% was included in all cases. Figure 2 shows the comparison of LCS proposed by Poling et al. and GCM of Constantinou for estimating the acentric factor for C_1-C_{12} n-alkanes, C_1-C_{10} 1-alcohols and C_4-C_5 methyl esters. The latter method is inapplicable for methane, hence that value was omitted from Fig. 2b. LCS suggested by Poling et al. provided better estimation, as GCM of Constantinou significantly underestimated ω for C_1-C_7 1-alcohols and slightly underestimated it for methyl esters. Moreover, ω of short-chain n-alkanes are slightly overestimated, shown in Fig. 2b.

Figures 3 and 4 show the GCM of Joback and Constantinou for T_{bn}, T_c, V_c, and p_c, respectively. Methods of Joback and of Constantinou are inapplicable for methane, because only group C can be applied for the calculations which is obviously insufficient and leads to improper estimations. Generally, the accuracy of both GCMs increases with the length of the carbon chain, as the agreement with reference data is better for higher values of T_c, V_c, and lower values of p_c, therefore, these methods may work for even longer-chain molecules as well. Note that the possibility for extrapolation depends on the range of molecules that was originally used to determine the group contributions for each method. If the range of original reference data was wide concerning molecular weight and chemical families as well, the method is more robust and universal. In case of the presently investigated chemical families, there are only a few different groups, thus the group contributions determined in the investigated methods were based on a broad dataset. For instance, in case of the method of Joback, original reference data for

Table 3 Availability of the reference data

	ω	T_{bn}	T_c	p_c	V_c	ρ_l	$c_{p,l}$	$c_{p,v}$	k_v	k_l	μ_v	H_{Tbn}	D_{12}
n-alkanes	C_1-C_{10} C_{12}												C_1-C_6
1-alcohols	C_1-C_{10}							C_1-C_5	–			C_1-C_6	C_1-C_2
methyl esters	C_4-C_5	C_3-C_{11} C_{13} C_{15} C_{17} $C_{19:0}$	C_3-C_6 C_{13}	C_3-C_6		C_3-C_7 C_9 C_{11} C_{13} C_{15} $C_{19:0}$ $C_{19:1}$	C_3-C_9 C_{11} C_{15}	C_3	–			C_3-C_5	C_3

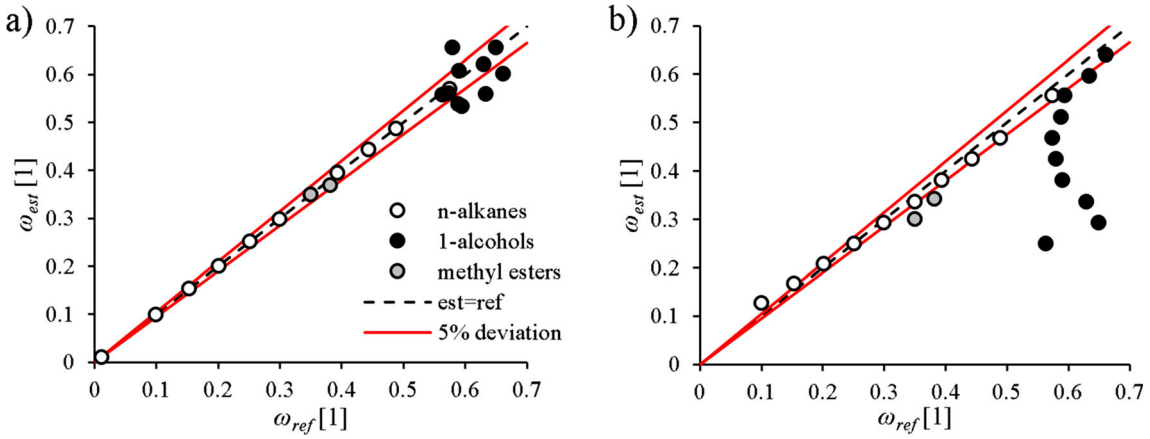

Fig. 2 Comparison of the acentric factor with the reference data by using LCS suggested by Poling et al. (**a**) and GCM of Constantinou (**b**)

determining the group contributions were available for the normal boiling point and critical properties up to n-eicosane, 1-eicosanol, and methyl butanoate for n-alkanes, 1-alcohols, and methyl esters, respectively. This may allow us to extrapolate within reasonable limits, if no further data are available. As an example, normal boiling points of methyl esters are estimated within 5% deviation shown in Fig. 3a, although no reference data were available for longer-chain methyl esters when group contributions were determined originally by Joback, demonstrating the justification of the possible extrapolation. GCM of Constantinou notably underestimates T_{bn} for longer-chain methyl esters, despite the good estimation for the

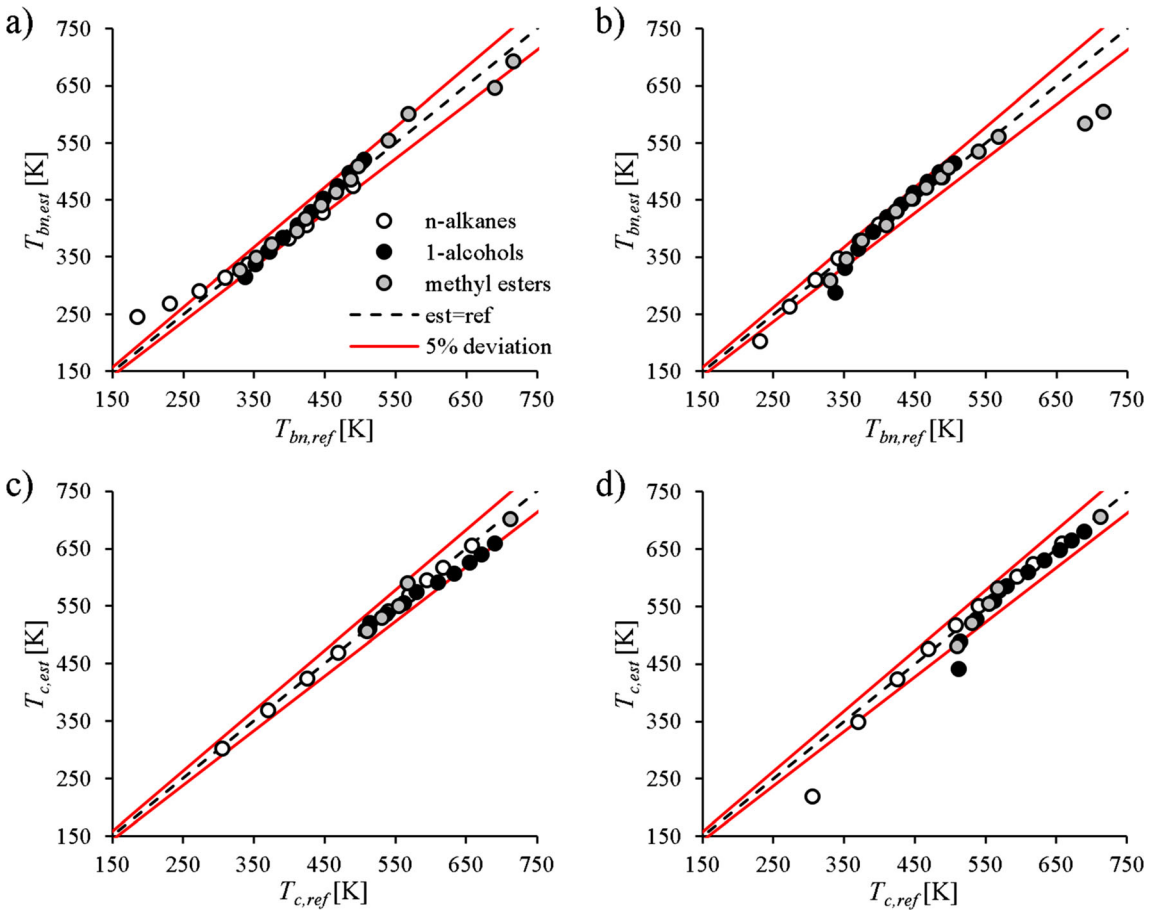

Fig. 3 Comparison of the atmospheric boiling temperature and the critical temperature with the reference data by using the method of Joback (**a**, **c**) and Constantinou (**b**, **d**). Higher T_{bn} and T_c values correspond to higher M

other molecule types. The deviation of T_{bn} of C_2-C_3 n-alkanes exceeds 5% by either approach, shown in Fig. 3a and b. The method of Constantinou notably underestimates T_{bn} and T_c of methanol, shown in Fig. 3b and d. However, both methods estimate V_c properly, shown in Fig. 4a and b. The method of Joback is superior for T_c and T_{bn} for all the investigated substances while the method of Constantinou provided a better estimation for p_c, shown in Fig. 4d, since the method of Joback highly overestimated this property of methyl esters, shown in Fig. 4c. The used optimization criterion for determining the group contributions for the estimating methods may result in the different accuracy for shorter- and longer-chain molecules. For instance, Joback [30, 31] minimized the sum of absolute deviations, which resulted in slightly higher errors for the outliers but provided better estimation for the majority of the compounds. In case of n-alkanes, ethane has a slightly different structure with only CH_3 groups, than the longer-chain molecules with only a difference in an additional CH_2 group. Methanol and methyl ethanoate have different structures in their own chemical family, as well. However, OH, COO, and CH_3COO groups have higher group contributions, than CH_2 and CH_3 groups, thus this effect is less considerable for 1-alcohols and methyl esters.

The critical parameter is unique for each material. Since the properties discussed next are functions of temperature and/or pressure, the markers were modified for better presentation. Figure 5 shows the comparison of the method of Joback and Nielsen for $c_{p,v}$ estimation of C_2-C_{12} n-alkanes, C_1-C_5 1-alcohols, and methyl ethanoate. Methane was excluded, as both methods are inapplicable. $c_{p,v}$ of methanol vapor could not be estimated properly by either methods for $T_r < 0.75$ since it is not monotonic at 1 bar, see Fig. 5c. From the boiling point to approximately 390 K, it decreases, then increases with temperature at $T > 390$ K. This behavior of methanol was investigated earlier by Weltner and Pitzer [61]. For the other investigated materials, $c_{p,v}$ increases with temperature. The method of Nielsen highly overestimates $c_{p,v}$ of methyl ethanoate while the method of Joback estimates that within 5% deviation except for $T_r > 2.35$, although no reference data were available for methyl esters when group contributions for $c_{p,v}$ were determined originally by Joback [30], which shows the robustness of the method. Therefore, the method of Joback performs better for $c_{p,v}$ estimation. Moreover, a correction function was introduced, only for methanol, for the method of Joback, in order to capture the non-monotonic behavior of $c_{p,v}$:

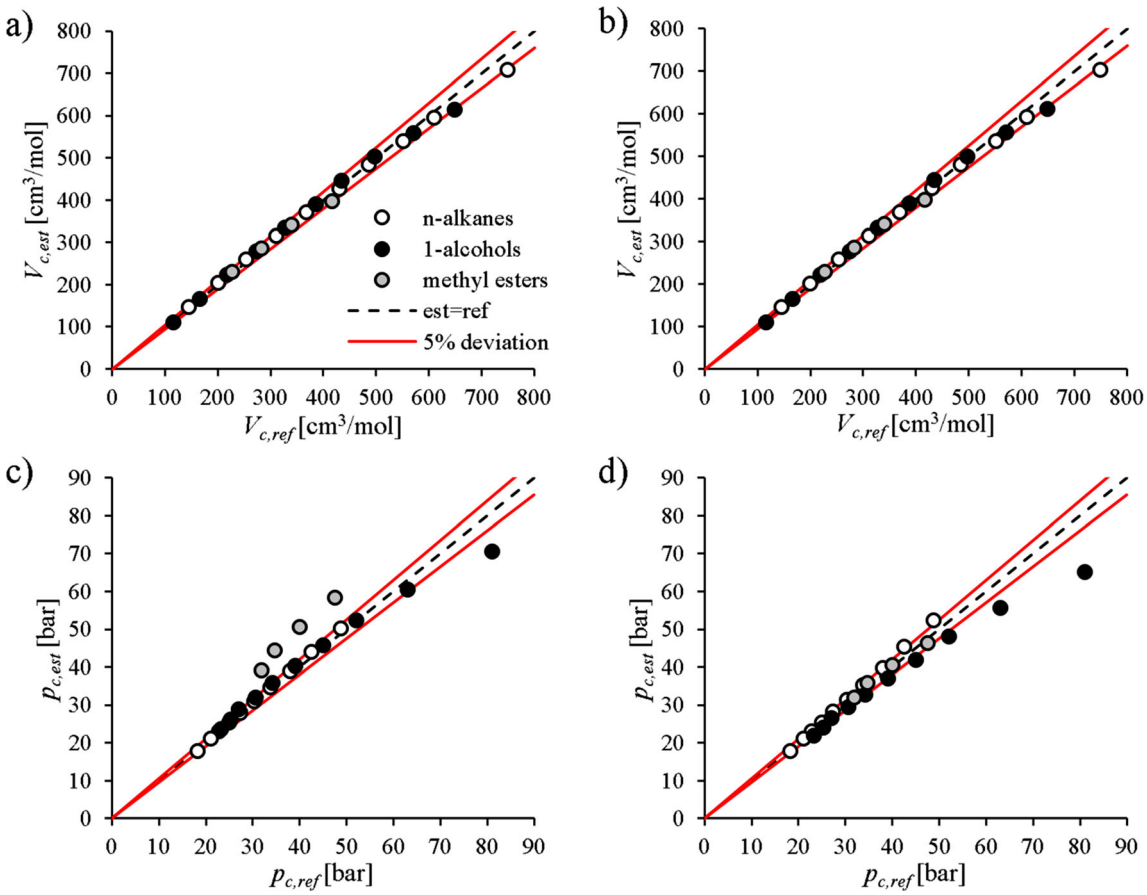

Fig. 4 Comparison of critical volume and critical pressure with the reference data by using the method of Joback (**a**, **c**) and Constantinou (**b**, **d**). Higher V_c and lower p_c values correspond to higher M

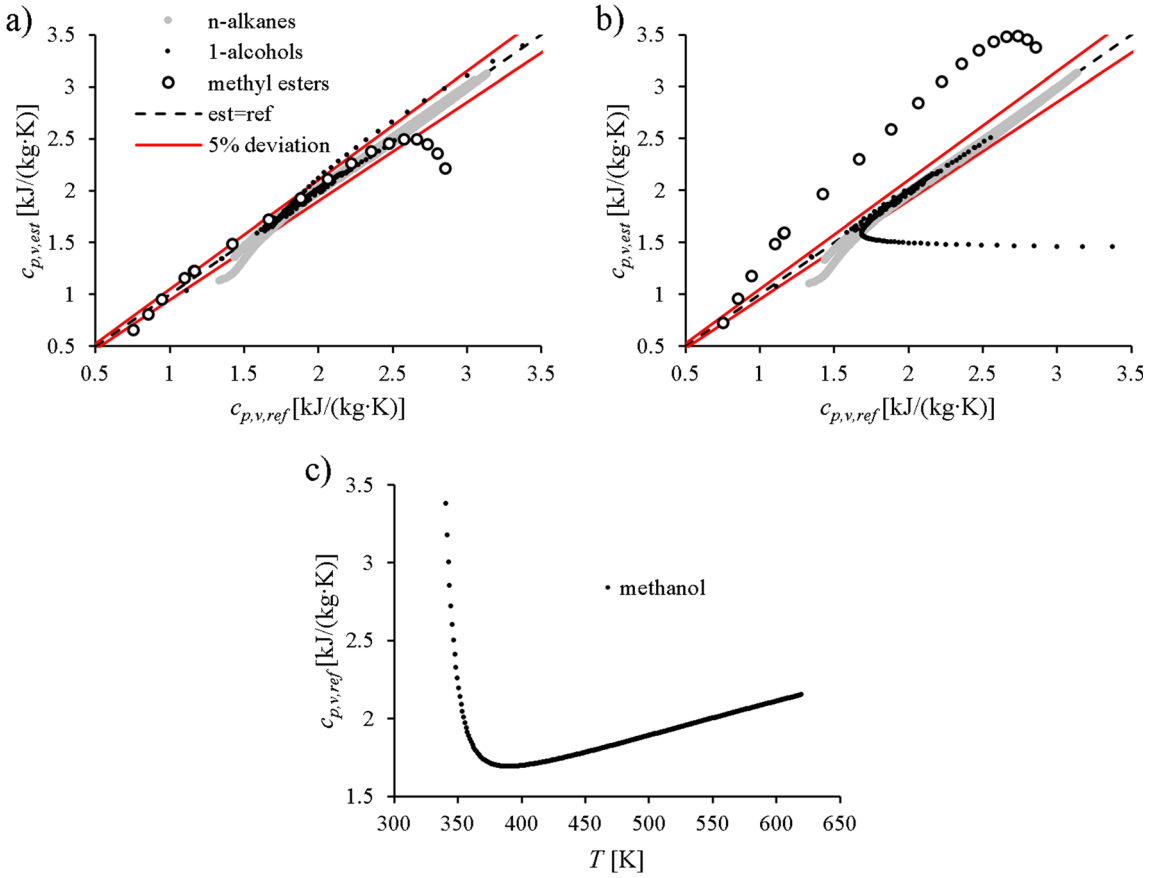

Fig. 5 Comparison of the temperature-dependent vapor specific heat capacity with reference data by using the method of Joback (**a**) and Nielsen (**b**), and reference data for methanol (**c**). Higher $c_{p,v}$ values correspond to a higher temperature for a given material, except for methanol, where $c_{p,v}$ is not monotonic at 1 bar

$$c_{p,v} = \left(4.428 \cdot 10^{12} \cdot e^{-43.34 \cdot T_r} + 1.0572 \cdot e^{-0.04294 \cdot T_r}\right) \cdot c_{p,v,Joback}, \tag{33}$$

where $c_{p,v,Joback}$ is the result of Eq. (12). The range of validity of Eq. (33) is $0.66 < T_r < 1.21$. Note that Fig. 5a shows the corrected $c_{p,v}$ values for methanol.

For $c_{p,l}$, a modified LCS method of Bondi and a GCM of Ruzicka are compared for C_2-C_{12} n-alkanes, C_1-C_{10} 1-alcohols, and C_3-C_{11} and C_{15} methyl esters. Note that ω and $c_{p,v}$ are input parameters for the modified LCS of Bondi, Eq. (15). As a consequence, $c_{p,v}$ was calculated with GCM of Joback

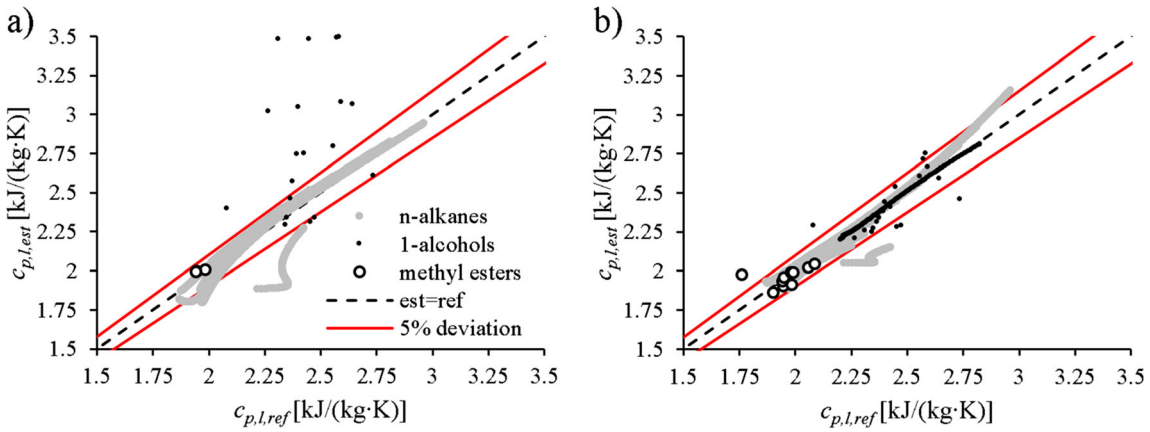

Fig. 6 Comparison of the temperature-dependent liquid-phase specific heat capacity with reference data by using the modified LCS of Bondi (**a**) and GCM of Ruzicka (**b**). Higher $c_{p,l}$ values correspond to a higher temperature for a given material, except for ethane, where $c_{p,l}$ is not monotonic at 1 bar

and Fig. 6a contains only those fluids, where ω was available as reference data. Methane was excluded from Fig. 6, as both GCM of Joback and GCM of Ruzicka are inapplicable. Generally, $c_{p,l}$ increases with temperature for the investigated fluids, except for ethane, which has a minimum at 1 bar. This non-monotonic behavior cannot be captured by either methods for ethane, shown in Fig. 6. Modified LCS of Bondi provided a highly inaccurate approximation for methanol, thus those values were omitted in Fig. 6a. Nevertheless, both methods provided an appropriate estimation for n-alkanes while the results of GCM of Ruzicka agree better with reference data in case of 1-alcohols and methyl esters. Consequently, the method of Ruzicka performed better in general. Note that $c_{p,l}$ of methanol had a non-unity slope and its $c_{p,l}$ was estimated within 5% deviation for $0.5 < T_r < 0.6$ by the GCM of Ruzicka. Fortunately, a correction function for Eq. (14) for only methanol was able to provide an excellent fit. This is the following:

$$c_{p,l} = \left(3.00424 \cdot e^{-2.00145 \cdot T_r} - 25.53 \cdot e^{-12.79 \cdot T_r}\right) \cdot c_{p,l,Ruzicka}, \quad (34)$$

where $c_{p,l,Ruzicka}$ is the result of Eq. (14). The range of validity of Eq. (34) is $0.34 < T_r < 0.66$. Both a third order polynomial and a two-term exponential fit worked well in the range of the available data, however, the exponential variant captured the trends even at the edges, as shown in Fig. 6b.

ρ_l was available for all the investigated fluids, however, reference data for μ_v, k_v, and k_l was only available for n-alkanes, therefore, the present evaluation is confined to them, and only the results of the best performing methods are presented. Generally, lower ρ_l, k_l, and higher μ_v, k_v values correspond to higher temperature for the investigated materials. Figure 7a and b show the comparison of ρ_l and μ_v with reference data. GCM of Elbro estimated liquid density excellently. However, it is not applicable for methane, thus it was excluded from Fig. 7a. Note that GCM of Elbro is not suitable for methanol, however GCM suggested by Baum, Eq. (25), provided proper estimation within 5% deviation for $0.34 < T_r < 0.66$, not shown here. LCS of Lucas is accurate for μ_v estimation, shown in Fig. 7b. Both the LCS method of Chung and the modified Eucken method, Eq. (20), provided an excellent

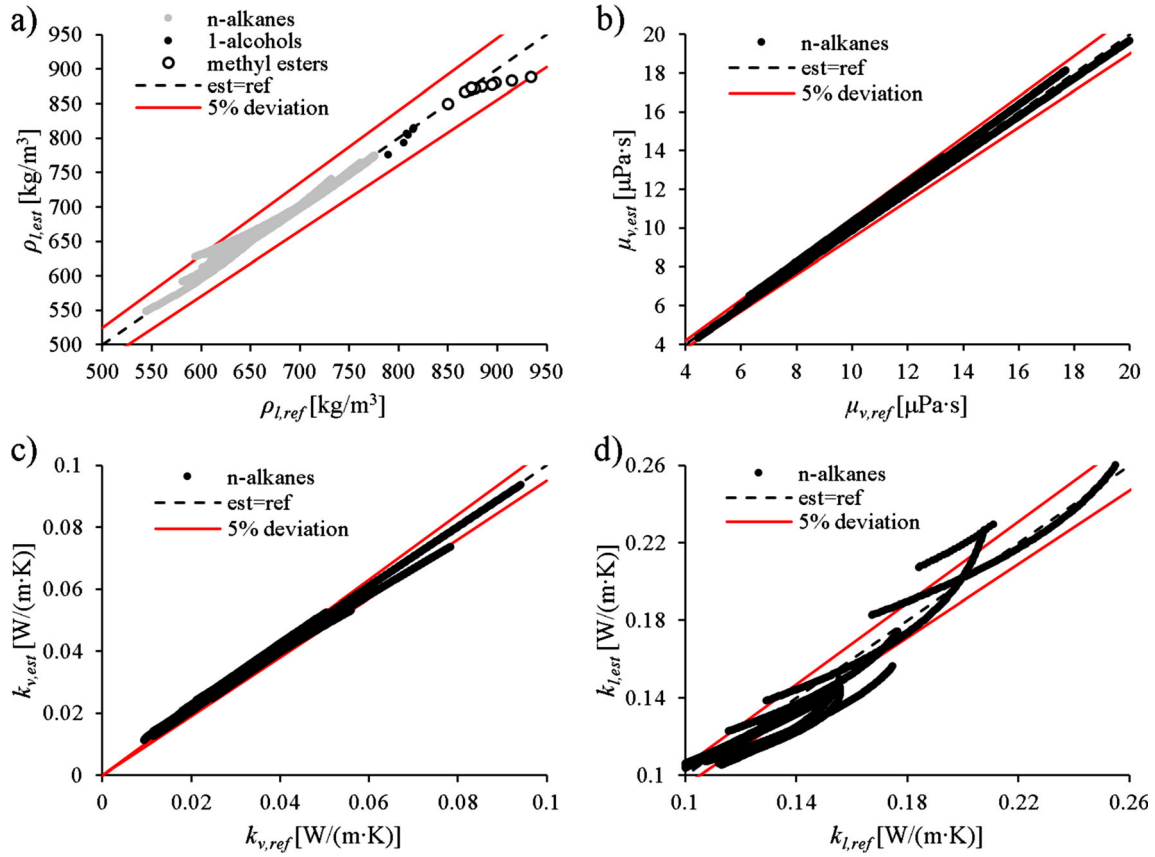

Fig. 7 Evaluation of GCM of Elbro for temperature-dependent liquid density (**a**), LCS of Lucas for temperature-dependent vapor viscosity (**b**), modified LCS Eucken method for temperature-dependent vapor (**c**), and GCM of Sastri for liquid (**d**) thermal conductivity estimation. Lower ρ_l, k_l and higher μ_v, k_v values correspond to a higher temperature for a given material

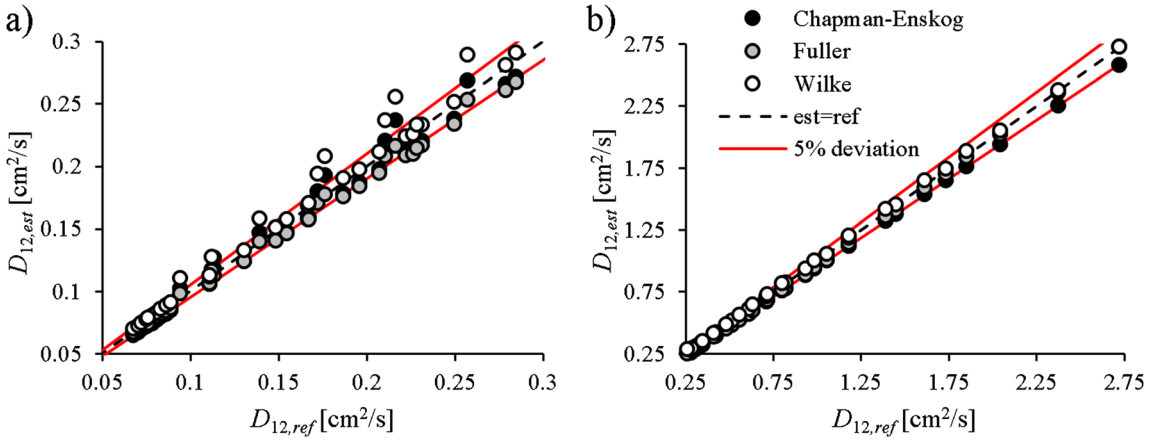

Fig. 8 Comparison of the classical Chapman-Enskog formula, method of Wilke, and method of Fuller for C_1-C_6 n-alkanes for estimating gas-phase mutual diffusion coefficient in nitrogen atmosphere

estimation for k_v while only the latter is presented in Fig. 7c. For k_l, GCMs of Sastri worked well, however, Eq. (23) failed to yield an acceptable temperature-dependent result. Eq. (24) provided a slightly better estimation for k_l, thus these results are shown in Fig. 7d.

As the gas-phase mutual diffusion coefficient is interpreted for two constituents, nitrogen was selected as a pair for all the investigated materials, as it is often used as an inert ambient gas in mass transfer experiments. Figure 8 shows the comparison of the classical Chapman-Enskog formula, the method of Wilke, and the method of Fuller for C_1-C_6 n-alkanes. The investigated D_{12} range is divided for better visualization, as there is an order of magnitude difference in the gas-phase mutual diffusion coefficient due to the temperature dependency. Based on the available reference data, the last model outperformed all the others in the presented range, even at high temperatures. Nevertheless, the classical Chapman-Enskog formula is widely used, even in the state-of-the-art numerical codes [62], although the method of Fuller requires more general input data of the constituents, which are broadly available in refs. [47, 48]. As D_{12} decreases with pressure, Fig. 9 shows the comparison of the former methods for methanol, ethanol, and methyl ethanoate at atmospheric and elevated pressure (up to 100 bar) conditions. For the latter case, the method of Fuller estimates D_{12} within ±10% deviation. For atmospheric pressure, method of Fuller estimates D_{12} of ethanol properly while it underestimates that of methanol. Generally, the deviation increases with temperature, which corresponds to higher D_{12} values. All the other methods provided even less accurate estimation for methanol.

As with the critical parameters, the enthalpy of vaporization at the normal boiling point is also unique for each material. Figure 10. shows the comparison of methods suggested by Riedel, Chen, and Vetere for C_1-C_{12} n-alkanes, C_1-C_6 1-alcohols, and C_3-C_5 methyl esters. In general, all of them provide sufficient estimation. However, LCS of Vetere slightly underestimates H_{Tbn} of 1-alcohols in the range of 400–700 kJ/kg. Therefore, LCS methods of Riedel and Chen are recommended.

Table 4 summarizes the average relative deviation (*ARD*) values for each of the investigated material property

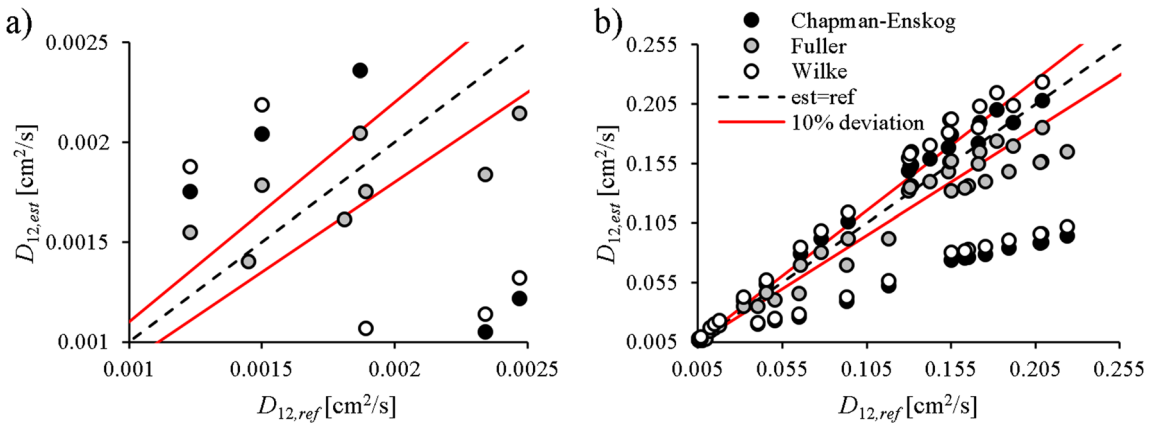

Fig. 9 Comparison of the classical Chapman-Enskog formula, method of Wilke, and method of Fuller for methanol, ethanol, and methyl ethanoate for estimating gas-phase mutual diffusion coefficient of vapor and nitrogen at elevated (up to 100 bar) (**a**) and atmospheric (**b**) pressure

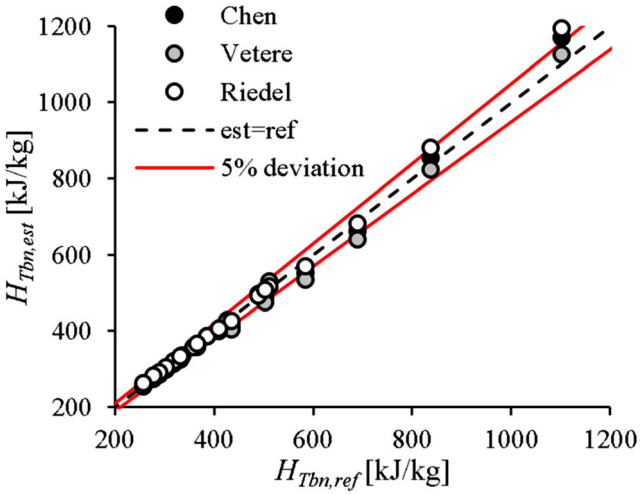

Fig. 10 Comparison of the LCS methods of Riedel, Chen, and Vetere for estimating the enthalpy of vaporization at the normal boiling point

estimation methods for all molecules, calculated by Eq. (35) to quantify the aforementioned evaluation:

$$ARD = \frac{\sum_{i=1}^{N} \frac{|calc_i - ref_i|}{ref_i}}{N}, \tag{35}$$

where N is the number of reference data points for a certain property, $calc_i$ is the calculated, while ref_i is the reference value, respectively.

5 Conclusions

Several formulae are available for estimating various thermodynamic properties of fuels since the available reference database is often limited. They are all based on the law of corresponding states (LCS) and the group contribution method (GCM) which are connected to molecular theory. Since none of the formulae are universal, numerous methods were evaluated in the present paper against reference data, leading to the following conclusions about their applicability for principally liquid fuel combustion applications.

1. LCS proposed by Poling et al. is recommended for calculating the acentric factor.
2. GCM of Joback is more universal and suitable for estimating atmospheric boiling temperature, specific heat capacity of the vapor-phase, and critical properties, except for p_c, where GCM of Constantinou is recommended. However, a correction function for GCM of Joback was introduced for $c_{p,v}$ of methanol for $0.66 < T_r < 1.21$.
3. For liquid-phase specific heat capacity, GCM of Ruzicka performed the best. A correction function was introduced for methanol only in order to estimate $c_{p,l}$ properly for $0.34 < T_r < 0.66$.
4. GCM of Elbro is applicable for estimating liquid density. For n-alkanes, the LCS method of Lucas estimates vapor

Table 4 Average relative deviation between calculated values and reference data. Superscripts: 1: n-alkanes, 2: 1-alcohols, 3: methyl esters, and 4: all the investigated materials

ω	**Poling**				**Constantinou**			
	0.3633%[1]	6.050%[2]	1.664%[3]	2.949%[4]	6.181%[1]	26.56%[2]	12.20%[3]	15.99%[4]
	Joback				**Constantinou**			
T_{bn}	7.764%[1]	2.482%[2]	2.303%[3]	3.962%[4]	6.049%[1]	3.906%[2]	4.395%[3]	4.737%[4]
T_c	0.2391%[1]	2.466%[2]	1.460%[3]	1.371%[4]	4.334%[1]	2.624%[2]	2.205%[3]	3.321%[4]
p_c	2.228%[1]	4.451%[2]	25.12%[3]	6.970%[4]	3.647%[1]	7.119%[2]	1.837%[3]	4.792%[4]
V_c	1.915%[1]	2.306%[2]	1.719%[3]	2.045%[4]	1.741%[1]	2.225%[2]	1.719%[3]	1.939%[4]
ρ_l	**Elbro**				**Baum**			
	0.7909%[1]	0.5961%[2]	1.322%[3]	0.7932%[4]	1.484%[1]	1.595%[2]	6.284%[3]	1.520%[4]
$c_{p,l}$	**Bondi**				**Ruzicka**			
	2.682%[1]	18.02%[2]	2.208%[3]	2.849%[4]	1.874%[1]	11.09%[2]	2.516%[3]	2.756%[4]
$c_{p,v}$	**Joback**				**Nielsen**			
	1.210%[1]	4.924%[2]	5.995%[3]	1.693%[4]	2.099%[1]	4.858%[2]	30.10%[3]	2.606%[4]
k_v	**Chung**				**Eucken (Eq. (19))**			
	4.494%[1]				15.71%[1]			
	Modified Eucken (Eq. (20))				**Stiel (Eq. (21))**			
	4.720%[1]				7.297%[1]			
k_l	**Latini**				**Sastri (Eq. (23))**			
	10.63%[1]				6.374%[1]			
	Sastri (Eq. (24))							
	5.291%[1]							
μ_v	**Chung**				**Lucas**			
	2.106%[1]				1.671%[1]			
H_{Tbn}	**Chen**				**Vetere**			
	0.2880%[1]	4.238%[2]	0.7349%[3]	1.540%[4]	1.021%[1]	5.370%[2]	2.014%[3]	2.474%[4]
	Riedel							
	1.064%[1]		3.336%[2]		0.5426%[3]		1.667%[4]	
D_{12}	**Chapman-Enskog**				**Fuller**			
	4.939%[1]	37.59%[2]	0.8522%[3]	18.44%[4]	3.439%[1]	13.35%[2]	10.80%[3]	7.688%[4]
	Wilke							
	3.722%[1]		40.31%[2]		7.248%[3]		19.06%[4]	

viscosity properly. As for thermal conductivity, the LCS method of Chung and the modified Eucken method for vapor-phase and GCM of Sastri for the liquid-phase are the best approaches.

5. Based on reference data for n-alkanes, methanol, ethanol, and methyl ethanoate in a nitrogen atmosphere, method of Fuller provided acceptable estimation for the gas-phase mutual diffusion coefficient.
6. LCS methods suggested by Riedel and Chen are suitable for determining the enthalpy of vaporization at the normal boiling point.

Funding Open Access funding provided by Budapest University of Technology and Economics. The research reported in this paper and carried out at the Budapest University of Technology and Economics has been supported by the National Research Development and Innovation Fund (TKP2020 National Challenges Subprogram, Grant No. BME-NCS) based on the charter of bolster issued by the National Research Development and Innovation Office under the auspices of the Ministry for Innovation and Technology and project №. OTKA-FK 124704, New National Excellence Program of the Ministry of Human Capacities project №.s ÚNKP-18-4-BME-195 and ÚNKP-18-3-I-BME-145, New National Excellence Program of the Ministry for Innovation and Technology project №.s ÚNKP-19-3-I-BME-236 and ÚNKP-19-4-BME-213, and the János Bolyai Research Scholarship of the Hungarian Academy of Sciences.

Declarations

Conflict of interest The authors declare that there is no conflict of interest.

References

1. Dunn JB (2019) Biofuel and bioproduct environmental sustainability analysis. Curr Opin Biotechnol 57:88–93. https://doi.org/10.1016/j.copbio.2019.02.008
2. Li Y, Tang W, Chen Y et al (2019) Potential of acetone-butanol-ethanol (ABE) as a biofuel. Fuel 242:673–686. https://doi.org/10.1016/j.fuel.2019.01.063
3. Lødeng R, Lunder O, Lein J-E et al (2018) Synthesis of light olefins and alkanes on supported iron oxide catalysts. Catal Today 299:47–59. https://doi.org/10.1016/j.cattod.2017.06.039
4. Deneyer A, Renders T, Van Aelst J et al (2015) Alkane production from biomass: chemo-, bio- and integrated catalytic approaches. Curr Opin Chem Biol 29:40–48. https://doi.org/10.1016/j.cbpa.2015.08.010
5. Mączyńska J, Krzywonos M, Kupczyk A et al (2019) Production and use of biofuels for transport in Poland and Brazil – the case of bioethanol. Fuel 241:989–996. https://doi.org/10.1016/j.fuel.2018.12.116
6. Alfonsín V, Maceiras R, Gutiérrez C (2019) Bioethanol production from industrial algae waste. Waste Manag 87:791–797. https://doi.org/10.1016/j.wasman.2019.03.019
7. Huang H, Liu Q, Teng W et al (2018) Improvement of combustion performance and emissions in diesel engines by fueling n-butanol/diesel/PODE3–4 mixtures. Appl Energy 227:38–48. https://doi.org/10.1016/j.apenergy.2017.09.088
8. Yusri IM, Mamat R, Akasyah MK et al (2019) Evaluation of engine combustion and exhaust emissions characteristics using diesel/butanol blended fuel. Appl Therm Eng 156:209–219. https://doi.org/10.1016/j.applthermaleng.2019.02.028
9. Devarajan Y, Munuswamy DB, Nagappan B, Pandian AK (2018) Performance, combustion and emission analysis of mustard oil biodiesel and octanol blends in diesel engine. Heat Mass Transf 54:1803–1811. https://doi.org/10.1007/s00231-018-2274-x
10. Prakash T, Geo VE, Martin LJ, Nagalingam B (2019) Evaluation of pine oil blending to improve the combustion of high viscous (castor oil) biofuel compared to castor oil biodiesel in a CI engine. Heat Mass Transf 55:1491–1501. https://doi.org/10.1007/s00231-018-2519-8
11. International Energy Agency (2021) Bioenergy - Fuels & Technologies. https://www.iea.org/fuels-and-technologies/bioenergy. Accessed 19 Jan 2021
12. International Energy Agency (2021) Transport Biofuels - Analysis. https://www.iea.org/reports/transport-biofuels. Accessed 19 Jan 2021
13. Lefebvre AH, McDonell VG (2017) Atomization and sprays, 2nd edn. CRC Press, Taylor & Francis Group, Boca Raton
14. Sazhin S (2014) Droplets and sprays
15. Saufi AE, Frassoldati A, Faravelli T, Cuoci A (2019) DropletSMOKE++: a comprehensive multiphase CFD framework for the evaporation of multidimensional fuel droplets. Int J Heat Mass Transf 131:836–853. https://doi.org/10.1016/j.ijheatmasstransfer.2018.11.054
16. Strizhak PA, Volkov RS, Castanet G et al (2018) Heating and evaporation of suspended water droplets: experimental studies and modelling. Int J Heat Mass Transf 127:92–106. https://doi.org/10.1016/j.ijheatmasstransfer.2018.06.103
17. Nomura H, Murakoshi T, Suganuma Y et al (2017) Microgravity experiments of fuel droplet evaporation in sub- and supercritical environments. Proc Combust Inst 36:2425–2432. https://doi.org/10.1016/j.proci.2016.08.046
18. Wang X, Dai M, Wang J et al (2019) Effect of ceria concentration on the evaporation characteristics of diesel fuel droplets. Fuel 236:1577–1585. https://doi.org/10.1016/j.fuel.2018.09.085
19. Ma X, Zhang F, Han K, Song G (2016) Numerical modeling of acetone–butanol–ethanol and diesel blends droplet evaporation process. Fuel 174:206–215. https://doi.org/10.1016/j.fuel.2016.01.091
20. Ni Z, Han K, Zhao C et al (2018) Numerical simulation of droplet evaporation characteristics of multi-component acetone-butanol-ethanol and diesel blends under different environments. Fuel 230:27–36. https://doi.org/10.1016/j.fuel.2018.05.038
21. Eckel G, Le Clercq P, Kathrotia T et al (2018) Entrained flow gasification. Part 3: insight into the injector near-field by large Eddy simulation with detailed chemistry. Fuel 223:164–178. https://doi.org/10.1016/j.fuel.2018.02.176
22. Csemány D, Józsa V (2017) Fuel Evaporation in an Atmospheric Premixed Burner: Sensitivity Analysis and Spray Vaporization. Processes:5. https://doi.org/10.3390/pr5040080

23. Poling BE, Prausnitz JM, O'Connell JP (2001) The properties of gases and liquids, 5th edn. McGraw-Hill, New York
24. Su W, Zhao L, Deng S (2017) Group contribution methods in thermodynamic cycles: physical properties estimation of pure working fluids. Renew Sust Energ Rev 79:984–1001. https://doi.org/10.1016/j.rser.2017.05.164
25. Tahami S, Movagharnejad K, Ghasemitabar H (2019) Estimation of the critical constants of organic compounds via a new group contribution method. Fluid Phase Equilib 494:45–60. https://doi.org/10.1016/j.fluid.2019.04.022
26. Felden A, Esclapez L, Riber E et al (2018) Including real fuel chemistry in LES of turbulent spray combustion. Combust Flame 193:397–416. https://doi.org/10.1016/j.combustflame.2018.03.027
27. Pitzer KS, Lippmann DZ, Curl RF et al (1955) The volumetric and thermodynamic properties of fluids. II. Compressibility factor, vapor pressure and entropy of Vaporization1. J Am Chem Soc 77:3433–3440. https://doi.org/10.1021/ja01618a002
28. Ambrose D, Walton J (1989) Vapour pressures up to their critical temperatures of normal alkanes and 1-alkanols. Pure Appl Chem 61:1395–1403
29. Constantinou L, Gani R, O'Connell JP (1995) Estimation of the acentric factor and the liquid molar volume at 298 K using a new group contribution method. Fluid Phase Equilib 103:11–22. https://doi.org/10.1016/0378-3812(94)02593-P
30. Joback KG (1984) A unified approach to physical property estimation using multivariate statistical techniques. Massachusetts Institute of Technology, Department of Chemical Engineering
31. Joback KG, Reid RC (1987) Estimation of pure-component properties from group-contributions. Chem Eng Commun 57:233–243. https://doi.org/10.1080/00986448708960487
32. Constantinou L, Gani R (1994) New group contribution method for estimating properties of pure compounds. AICHE J 40:1697–1710. https://doi.org/10.1002/aic.690401011
33. Nielsen TL (1998) Molecular structure based property prediction. 15-point project Department of Chemical Engineering, Technical University of Denmark, Lyngby, DK-2800
34. Ruzicka V, Domalski E (1993) Estimation of the heat capacities of organic liquids as a function of temperature using group Additivity II.: compounds of carbon, hydrogen, halogens, nitrogen, oxygen, and sulfur. J Phys Chem Ref Data 22:619–657
35. Bondi AA (1968) Physical properties of molecular crystals, liquids, and glasses (Wiley series on the science and technology of materials). Wiley, New York
36. Chung TH, Lee LL, Starling KE (1984) Applications of kinetic gas theories and multiparameter correlation for prediction of dilute gas viscosity and thermal conductivity. Ind Eng Chem Fundam 23:8–13. https://doi.org/10.1021/i100013a002
37. Chung TH, Ajlan M, Lee LL, Starling KE (1988) Generalized multiparameter correlation for nonpolar and polar fluid transport properties. Ind Eng Chem Res 27:671–679. https://doi.org/10.1021/ie00076a024
38. Lucas K (1981) Die Druckabhängigkeit der Viskosität von Flüssigkeiten – eine einfache Abschätzung. Chemie Ing Tech 53:959–960. https://doi.org/10.1002/cite.330531209
39. Svehla RA (1962) Estimated viscosities and thermal conductivities of gases at high temperatures. NASA tech. Rept. R-132, Lewis research center, Cleveland
40. Stiel LI, Thodos G (1964) The thermal conductivity of nonpolar substances in the dense gaseous and liquid regions. AICHE J 10:26–30. https://doi.org/10.1002/aic.690100114
41. Latini G, Pacetti M (1978) The thermal conductivity of liquids — a critical survey, pp 245–253
42. Sastri SRS, Rao KK (1999) A new temperature–thermal conductivity relationship for predicting saturated liquid thermal conductivity. Chem Eng J 74:161–169. https://doi.org/10.1016/S1385-8947(99)00046-7
43. Sastri SRS, Rao KK (1993) Quick estimating for thermal conductivity
44. Baum EJ (1997) Chemical property estimation: theory and application. CRC Press, New York
45. Elbro HS, Fredenslund A, Rasmussen P (1991) Group contribution method for the prediction of liquid densities as a function of temperature for solvents, oligomers, and polymers. Ind Eng Chem Res 30:2576–2582. https://doi.org/10.1021/ie00060a011
46. Wilke CR, Lee CY (1955) Estimation of diffusion coefficients for gases and vapors. Ind Eng Chem 47:1253–1257. https://doi.org/10.1021/ie50546a056
47. Fuller EN, Schettler PD, Giddings JC (1966) New method for prediction of binary gas-phase diffusion coefficients. Ind Eng Chem 58:18–27. https://doi.org/10.1021/ie50677a007
48. Fuller EN, Ensley K, Giddings JC (1969) Diffusion of halogenated hydrocarbons in helium. The effect of structure on collision cross sections. J Phys Chem 73:3679–3685. https://doi.org/10.1021/j100845a020
49. Watson KM (1931) Prediction of critical temperatures and heats of vaporization. Ind Eng Chem 23:360–364. https://doi.org/10.1021/ie50256a006
50. Riedel L (1954) Kritischer Koeffizient, Dichte des gesättigten Dampfes und Verdampfungswärme Untersuchungen über eine Erweiterung des Theorems der übereinstimmenden Zustände Teil III. Chemie Ing Tech 26:679–683. https://doi.org/10.1002/cite.330261208
51. Chen NH (1965) Generalized correlation for latent heat of vaporization. J Chem Eng Data 10:207–210. https://doi.org/10.1021/je60025a047
52. Vetere A (1979) New correlations for predicting vaporization enthalpies of pure compounds. Chem Eng J 17:157–162. https://doi.org/10.1016/0300-9467(79)85008-X
53. Lemmon EW, McLinden MO, Friend DG (2019) Thermophysical properties of fluid systems, NIST Chemistry WebBook, NIST Standard Reference Database Number 69
54. National Library of Medicine of the National Institutes of Health - National Center for Biotechnology Information - PubChem Database. (2019). https://pubchem.ncbi.nlm.nih.gov. Accessed 3 Dec 2019
55. Winkelmann J (2007) Landolt-Börnstein - Group IV Physical Chemistry, p 474
56. National Oceanic and Atmospheric Administration's Office of Response and Restoration - Cameo Chemicals Database of Hazardous Materials. https://cameochemicals.noaa.gov/. Accessed 11 Jun 2020
57. National Library of Medicine of the National Institutes of Health - Hazardous Substances Data Bank (HSDB). https://www.nlm.nih.gov/toxnet/index.html. Accessed 11 Jun 2020
58. You X, Egolfopoulos FN, Wang H (2009) Detailed and simplified kinetic models of n-dodecane oxidation: the role of fuel cracking in aliphatic hydrocarbon combustion. Proc Combust Inst 32:403–410. https://doi.org/10.1016/j.proci.2008.06.041
59. Zhou D, Yang W, Li J, Tay KL (2016) Simplified fuel cracking process in reduced mechanism development: PRF – PAH kinetic models for combustion and soot prediction. Fuel 182:831–841. https://doi.org/10.1016/j.fuel.2016.06.053

60. Csemány D, Gujás I, Chong CT, Józsa V (2021) Thermophysical properties of n-alkanes, 1-alcohols, and methyl esters. https://doi.org/10.5281/ZENODO.4453074
61. Weltner W, Pitzer KS (1951) Methyl alcohol: the entropy, heat capacity and polymerization Equilibria in the vapor, and potential barrier to internal rotation. J Am Chem Soc 73:2606–2610. https://doi.org/10.1021/ja01150a053
62. Ansys Fluent Theory Guide 2020 R1 (2020)